Selective Activation of the Thyroid Hormone Receptor Beta (TRβ) Induces Tumor Suppression and Increases Efficacy of Therapeutic Agents

Noelle Gillis, PhD[1,2,3], Lauren Cozzens, BS[1,4], Emily Wilson, BS[1,5], Jennifer Tomczak, MPH[1], Eric Bolf, PhD[1,2,6], Frances Carr, PhD[1,2**]

[1] *Department of Pharmacology, Larner College of Medicine, Burlington, Vermont*

[2] *University of Vermont Cancer Center, Burlington, Vermont*

[3] *Current address: Masonic Cancer Center, University of Minnesota, Minneapolis, Minnesota*

[4] *Current address: University of Colorado, Anschutz Medical Campus, Aurora, Colorado*

[5] *Current address: University of Utah, Salt Lake City, Utah*

[6] *Current address: 2seventy Bio, Cambridge Massachusetts*

[**] *Corresponding author,* Email: frances.carr@med.uvm.edu

Short title: TRβ agonist blunts tumor progression and enhances therapies

Keywords: GC-1, Sobetirome, thyroid hormone receptor, anaplastic thyroid cancer

Noelle Gillis, gilli431@umn.edu; University of Minnesota, Minneapolis MN, 55455

Lauren Cozzens, lauren.cozzens@cuanschutz.edu; University of Colorado at Anschutz, Aurora, CO 80045

Emily Wilson, u1414297@utah.edu, University of Utah, Salt Lake City, UT 84116

Jennifer Tomczack, jennifer.tomczak@uvm.edu; University of Vermont College of Medicine, Pharmacology, Burlington, VT, 05405 USA; 802-656-9617

Eric Bolf, eric.bolf@2seventybio.com, Cambridge MA 02142

Frances Carr, frances.carr@med.uvm.edu; University of Vermont College of Medicine, Pharmacology, Burlington, VT, 05405 USA; 802-656-6318

The authors declare no potential conflicts of interest.

38 **Abstract**

39 Thyroid hormone receptor beta (TRβ) is a recognized tumor suppressor in numerous solid
40 cancers. The molecular signaling of TRβ has been elucidated in several cancer types
41 through re-expression models. Remarkably, the potential impact of selective activation of
42 endogenous TRβ tumor progression remains largely unexplored. We used cell-based
43 and *in vivo* assays to evaluate the effects of the TRβ agonist sobetirome (GC-1) on a
44 particularly aggressive and dedifferentiated cancer, anaplastic thyroid cancer (ATC).
45 Here we report that GC-1 reduced tumorigenic phenotypes, decreased cancer stem-like
46 cell population, and increased the efficacy of current therapeutics. GC-1 induced re-
47 differentiation of the ATC cells and increased sodium-iodide transporter (NIS) expression
48 and restored iodide uptake. GC-1 alone was as effective as Sorafenib in blunting tumor
49 growth *in vivo*. These results indicate that selective activation of TRβ not only induces a
50 tumor suppression program *de novo* but enhances the effectiveness of anti-cancer
51 agents.

52

53 ***Statement of Significance:*** Selective activation of TRβ reduces aggressive cancer cell
54 phenotype, cancer stem cell population, tumor growth and increases the efficacy of
55 current therapeutics. TRβ is a novel diagnostic biomarker and therapeutic target.

56 **INTRODUCTION**

57 There is compelling evidence that the nuclear receptor thyroid hormone receptor
58 beta (TRβ) is a suppressor of tumor progression, invasion, and metastases in multiple
59 solid tumors including thyroid, breast, colon and other cancers(1). Cell-based and animal
60 studies reveal that liganded TRβ induces apoptosis, reduces an aggressive phenotype,
61 decreases cancer stem cell populations, and slows tumor growth through modulation of
62 a complex transcriptional network (2-9) . Transcriptional regulation by TRβ is critical for
63 its function as a tumor suppressor because it acts as both a signal transducer and
64 facilitator of long-term epigenetic programming for maintenance of cell identity. Our recent
65 studies revealed that TRβ in the presence of triiodothyronine (T_3) induced a tumor-
66 suppressive transcriptomic program and cell redifferentiation in aggressive thyroid and
67 breast cancer cells (2,10). We identified several key mechanisms by which activation of
68 TRβ could reduce tumor progression, implicating thyroid hormone signaling as a
69 therapeutic opportunity in advanced cancers. Recent studies in breast (8), colon (11), and
70 liver (5) cancers also emphasize this untapped therapeutic potential (12,13).

71 Thyroid hormones, thyromimetics and their metabolites can activate TRα as well
72 as TRβ. Yet, the use of non-selective TRβ ligands, such as T_3, is problematic as a
73 therapeutic approach due to the adverse side-effects of hyperthyroidism and the potential
74 for cardiovascular events as a result of aberrant TRα activity. To subvert these negative
75 side effects, TRβ-selective thyromimetics have been developed (14,15). Several of these
76 drugs have been shown to be effective for treatment of metabolic and neurodegenerative
77 disorders in clinical trials(15). In particular, the TRβ agonist sobetirome (GC-1)

78 preferentially binds to and activates TRβ and induces the same transcriptomic response
79 as T_3 (15, 16) and has been successful in early clinical trials for treatment of dyslipidemia
80 (16-19). Despite their potential benefits demonstrated by numerous preclinical studies,
81 TRβ agonists remain untested as cancer therapeutics as single agents or in combination
82 with other treatments.

83 Here, we investigated the potential impact of a selective TRβ agonist in an
84 aggressive thyroid cancer model. The global incidence of thyroid cancer is increasing
85 faster than any other solid tumor (20,21). While prognoses for patients with differentiated
86 tumors receiving standard therapies are generally very good, outcomes for patients with
87 resistant or recurrent disease and poorly differentiated thyroid cancers (PDTC) are
88 extremely poor (22). Due to a lack of effective therapies, patients with advanced or
89 metastatic anaplastic thyroid cancer (ATC) have a higher mortality rate than all other
90 endocrine cancers combined (23). ATC tumors are refractory to radioiodine therapy due
91 to loss of the sodium-iodide symporter (NIS) expression, and traditional chemotherapy is
92 of limited benefit.

93 Activation of phosphatidylinositol 3-kinase (PI3K)–Akt–mammalian target of
94 rapamycin (mTOR) pathway (PI3K-Akt) and mitogen-activated protein kinase (MAPK)
95 signaling are recognized drivers of thyroid oncogenesis and blocking this activity is a
96 therapeutic focus. Yet inhibitors of the major components of these signaling cascades
97 rarely provide a durable response as resistance quickly develops. Current molecular
98 diagnostics provide a rationale for intervention with combination therapies (24). However,
99 combination treatments have not yielded significantly improved responses due to

100 development of resistance, and there are still no curative options (14). Therefore, there
101 remains an urgent need for innovative and less toxic therapeutics for ATC (25-27).

102 In our studies we establish the effects of GC-1 alone and in combination with
103 therapeutic agents in ATC cells with diverse genetic backgrounds (28). GC-1 alone
104 decreases the aggressive phenotype and increases the effectiveness of MAPK, PI3K,
105 and cell cycle inhibitors. GC-1 significantly increases expression of thyroid-specific genes,
106 inducing re-differentiation in ATC cells. Importantly, we observe an increase in NIS protein
107 which leads to enhanced iodide uptake implicating potential restoration of functionality.
108 Finally, GC-1 alone reduced tumor growth of ATC cells in xenografts as effectively as
109 Sorafenib. The combination of GC-1 and Sorafenib maximally suppressed tumor growth.
110 These observations indicate that activation of TRβ with isomer-selective agonists may be
111 an effective and practical adjuvant therapeutic strategy.

112 **RESULTS**

113 **GC-1 blocks the tumorigenic phenotype of ATC cells transduced with TRβ.**

114 We previously demonstrated that T_3 (10 nM) treatment of transduced SW1736
115 cells, in which TRβ is re-expressed (SW-TRβ), induced a tumor suppression
116 transcriptomic program and reduced cell growth when compared to cells transduced with
117 empty vector (SW-EV) (2). We therefore tested the ability of GC-1 (10 nM) to reduce ATC
118 phenotypes. We found that GC-1 similarly decreased cell growth in four days (**Fig. 1A**).
119 There was a 50% reduction in the overall growth rate of SW-EV cells and 75% reduction
120 in SW-TRβ cells (**Fig. 1B**), indicating potent activation of endogenous TRβ. There was
121 also a modest decrease in the cell migration rate of upon treatment with GC-1 (**Fig. 1C**).

As cancer stem cells are thought to be responsible for tumor initiation and recurrence, targeting these cells is key to successful treatment. Therefore, we tested whether thyroid cancer stem cells are responsive to GC-1. Thyrosphere formation is robust in SW-EV cells, and GC-1 induced a significant reduction in growth (**Fig. 1D**). Re-expression of TRβ (SW-TRβ) reduces thyrosphere growth and addition of GC-1 reduces thyrosphere formation by approximately 80% (**Fig. 1D**). These results indicate that GC-1 can activate TRβ to reduce the thyroid cancer stem cell population.

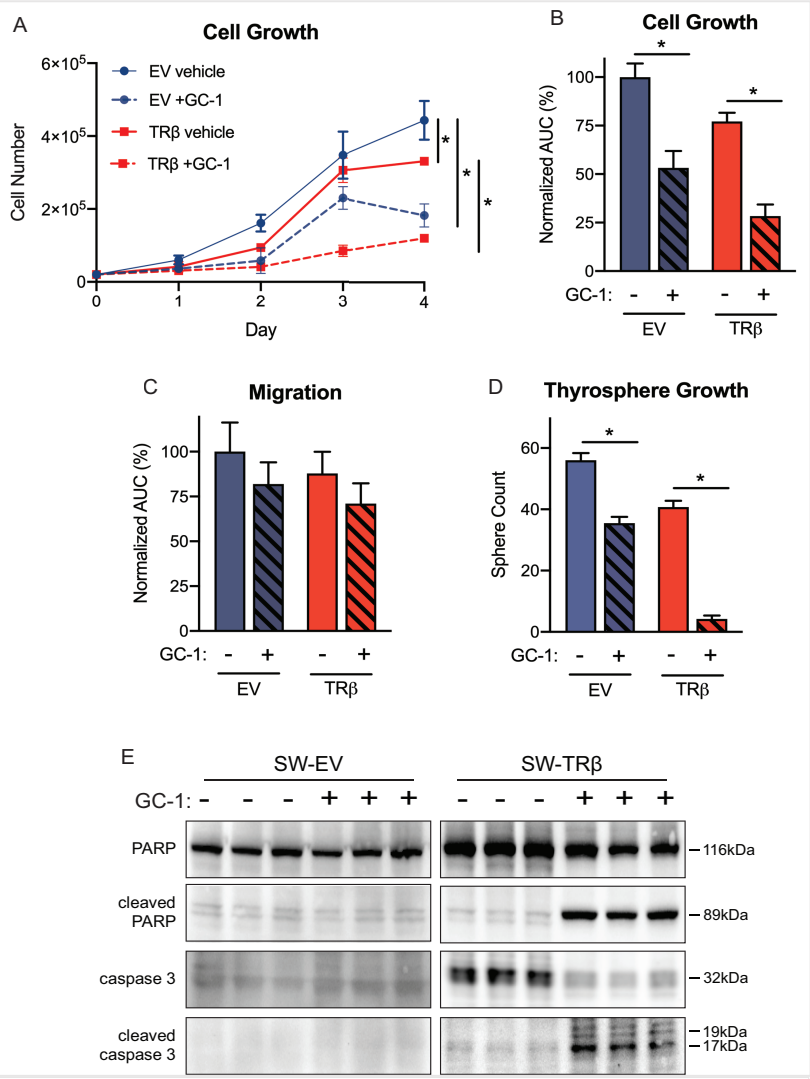

Figure 1. GC-1 blocks tumorigenic phenotypes in ATC cells transduced with TRβ. A. Growth curves demonstrate that SW-TRβ growth is significantly decreased after treatment with GC-1 for 4 days (n=3). Significance (* $p<0.05$) was determined by a two-way ANOVA and Tukey's multiple comparisons test. **B**. Area under the curve (AUC) analysis of growth curve data. Significance (* $p<0.05$) was determined by t-test. **C.** Treatment with GC-1 slows migration of SW-TRβ and SW-EV cells measured by scratch assay. Significance (* $p<0.05$) was determined by t-test. D. GC-1 repressed thyrosphere formation in SW-TRβ and SW-EV cells (n=4). Significance (* $p<0.05$) was determined by t-test. E. Immunoblot demonstrates that 5 days of GC-1 treatment induces apoptosis in SW-TRβ cells assessed by cleavage of PARP and caspase 3 (n=3).

145 Apoptotic signaling is central to ligand-activated TRβ modulation of the ATC
146 aggressive phenotype (2). Thus, we assessed the effects of GC-1 on PARP and caspase
147 3 cleavage by immunoblot as markers of late-stage apoptosis (**Fig. 1E**). GC-1 significantly
148 increased cleavage of PARP and caspase 3 in SW-TRβ consonant with increased
149 apoptotic signaling. Combined, these results indicate that GC-1 can activate TRβ to
150 reduce the aggressive phenotype in transduced ATC cells with TRβ re-expressed and
151 recapitulate effects seen with T_3 at comparable concentrations.

152 **GC-1 slows growth of parental ATC cells.**

153 Once we confirmed that GC-1 induces the same phenotypic changes in our
154 transduced ATC cell line model, it was critical to assess whether selective activation of
155 endogenous TRβ would induce similar effects in unmodified ATC cell lines (28). SW1736,
156 8505C, OCUT2, and KTC-2 cells all harbor *BRAF*^{V600E} and *TERT* driver mutations, but
157 otherwise have diverse mutational backgrounds (summarized in **Fig. 2A**). Endogenous
158 TRβ expression is low in all four ATC cell lines when compared with normal thyroid cells
159 (29). Treatment of each cell line with 10 nM GC-1 for four days yielded a modest but
160 significant decrease in cell growth (**Fig. 2B-E**). Treatment with 10 nM T_3 did not alter
161 growth of any of the cell lines. This result suggests that even low levels of endogenous
162 TRβ can be selectively activated with GC-1, and GC-1 is more effective at promoting
163 tumor suppressor activity than T_3.

164

A

Gene Function	Gene Name	Cell Line: SW1736	8505C	OCUT-2	KTC-2
		Mutation Type			
MAPK Signaling	BRAF	V600E	V600E	V600E	V600E
Telomerase	TERT (promoter)	124C-T	146C-T	146C-T	124C-T
DNA Homeostasis	TP53	Trunc.	Miss.		
PI3K Signaling	PIK3CA			Kinase Domain	
Cell-Cell Contact	NF2		Trunc.		
DNA Homeostasis	ATM		Trunc.		
TSH Signaling	TSHR	Miss.			
Histone Methyltransferase	KMT2C				Miss.
Histone Methyltransferase	KMT2D				Trunc.
Histone Acetyltransferase	EP300	Trunc.			
SWI/SNF Complex	ARID1A				In Frame
SWI/SNF Complex	SMARCA4		Miss.		

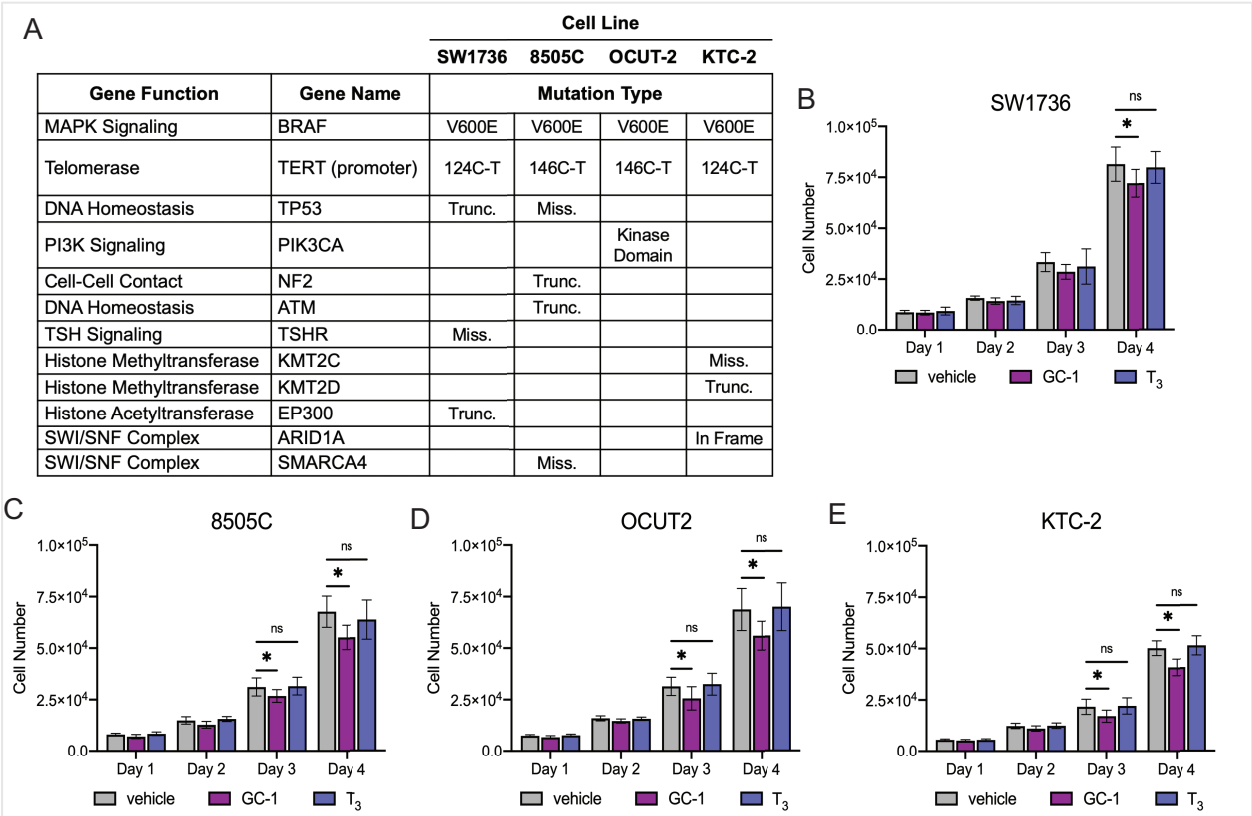

Figure 2: GC-1 slows growth of parental ATC cells. A. Summary of mutated genes in four ATC cell lines implemented in this study (17). B-E. Relative cell growth of unmodified ATC cell lines was measured by cell counting assay after 4 days of treatment with 10 nM GC-1 or 10 nM T_3. Significance (* $p<0.05$) was determined by a two-way ANOVA followed by Dunnett's multiple comparisons test; 3 independent experiments were performed per treatment group.

GC-1 increases the efficacy of selected therapeutic agents

Based on our previous work on activation of TRβ in ATC cells, we hypothesized that GC-1 could enhance the efficacy of therapeutics that target selective pathways. Cell viability was calculated following treatment for three days with increasing concentrations of the PI3K inhibitor Buparlisib (pan-PI3K inhibitor) or Alpelisib (PI3Kα mutant inhibitor) for OCUT2 cells which harbor a gain-of-function *PIK3CA* mutation (**Fig. 3A**), the cell cycle inhibitor Palbociclib (**Fig. 3B**), or the multi-tyrosine kinase inhibitor Sorafenib (**Fig. 3C**), with or without 10 nM GC-1. Each therapeutic agent decreased cell viability in three days

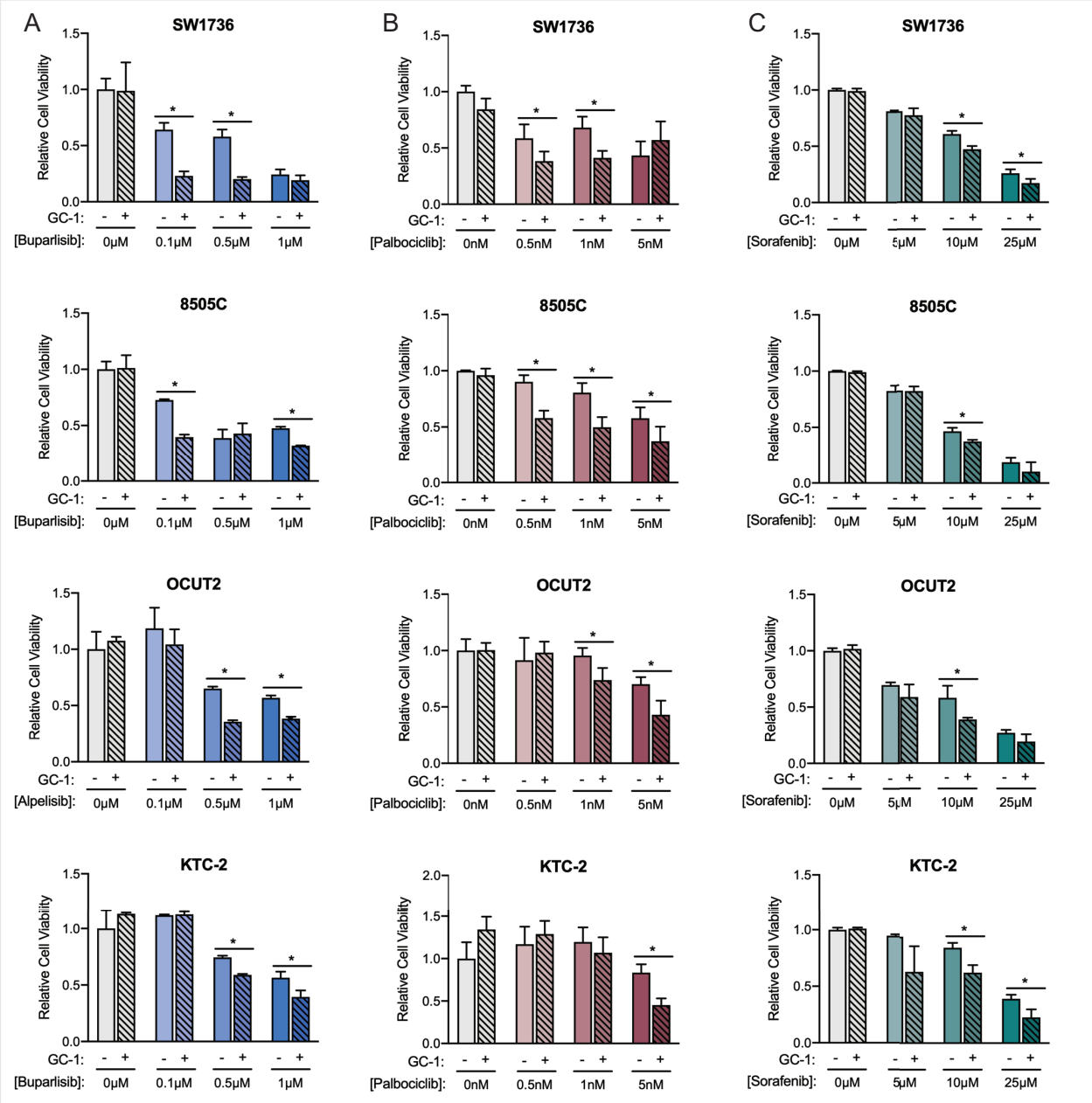

Figure 3. GC-1 increases efficacy of inhibitors. Cell viability of unmodified ATC cell lines was measured by SRB assay after 3 days of treatment with increasing concentrations buparlisib or alpelisib (A), sorafenib (B), or palbociclib (C) simultaneously in combination with 10 nM GC-1. Significance (* $p<0.05$) was determined by a two-way ANOVA followed by Sidak's multiple comparisons test; 3 independent experiments were performed per each treatment group.

173 in a dose-dependent manner. The addition of GC-1 significantly increased the efficacy of

174 these agents at lower concentrations. For example, 1 μM Buparlisib was required to

175 reduce cell viability below 50% in the absence of GC-1, but when combined with 10 nM
176 GC-1 this could be achieved with 0.1-0.5 μM Buparlisib (**Fig. 3A**). Similar trends were
177 observed with all four therapeutics and across the panel of cell lines used.

178 **GC-1 enhances the effects of therapeutic agents on cell migration**

179 In addition to reducing cell viability, many therapeutics target pathways that are
180 involved in cell migration. To further evaluate the ability of GC-1 to enhance the efficacy
181 of select therapeutics, cells were treated with the indicated inhibitors at concentrations
182 determined to be effective based on cell viability assays (**Fig. 3**), and migration was
183 observed by assessing wound closure. Each inhibitor was able to successfully slow
184 migration, and this effect was increased when each of the inhibitors were combined with
185 GC-1, except for Buparlisib in KTC-2 cells (**Fig. 4B-E**). Notably, GC-1 alone was able to
186 prevent wound closure of all cell lines with similar success as each inhibitor alone (**Fig.**
187 **4A-E**). These findings are similar to what we previously observed in experiments using
188 endogenous thyroid hormone, T_3, indicating GC-1 is a suitable alternative for TRβ
189 activation for slowing migration.

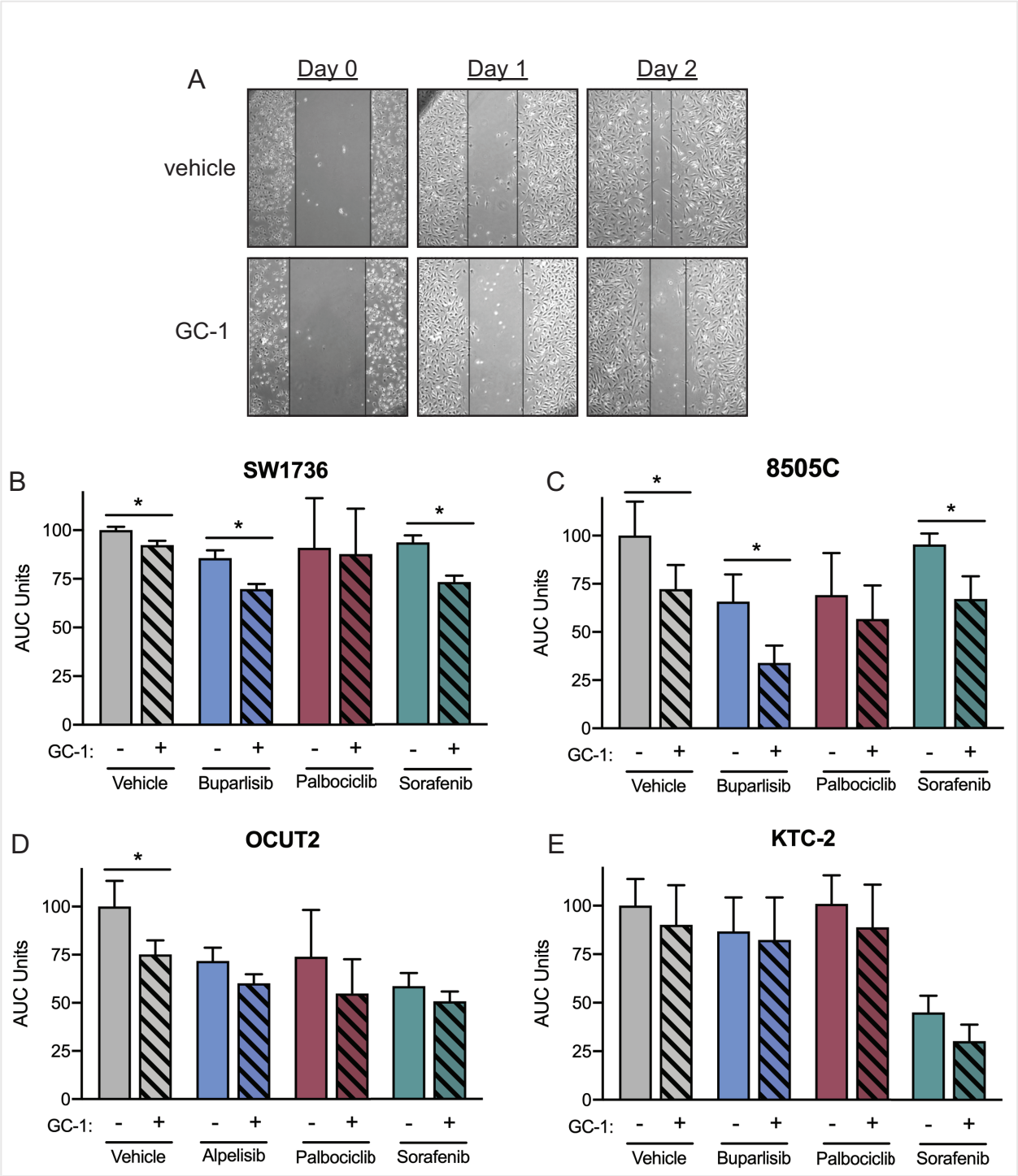

Figure 4. GC-1 enhances the effects of inhibitors on cell migration. Cell migration was measured by scratch assay. Representative images demonstrate reduced scratch closure after two days when ATC cells are treated with GC-1 (A). Area under the curve (AUC) analysis shows SW1736 (B), 8505C (C), OCUT2 (D), and KTC-2 (E) cells all exhibit lower rates of scratch closer after treatment with GC-1 alone and further reduced scratch closure rates after combined treatment with GC-1 and inhibitors. Significance (* $p<0.05$) was determined by t-test.

191 **GC-1 blocks tumorsphere outgrowth and increases efficacy of therapeutic agents.**

192 Current treatment options for ATC primarily target hyperproliferative cells, but
193 aggressive cancers like ATC are enriched for long-lived cancer stem cells that are thought
194 to be a major mechanism for therapy resistance and tumor recurrence. We previously
195 demonstrated that ligand-activated TRβ regulates genes related to stemness in ATC cells
196 and that GC-1 could block thyrosphere outgrowth in our modified ATC cells (**Fig. 1D**). We
197 therefore tested the hypothesis that GC-1 could prevent thyrosphere outgrowth after an
198 initial treatment with an inhibitor that targets proliferation.

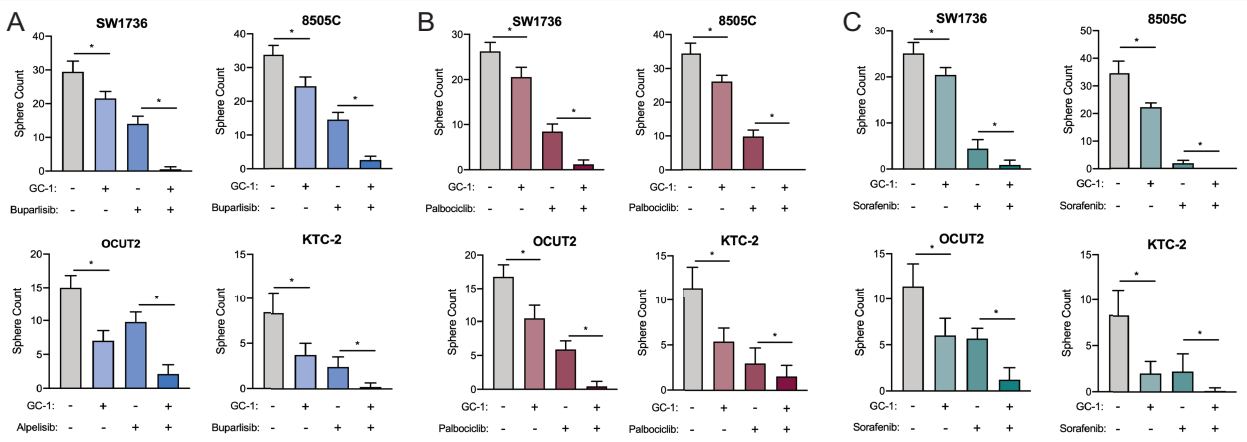

Figure 5. GC-1 blocks thyrosphere outgrowth and increases the efficacy of therapeutic agents. Thyrosphere growth was determined for ATC cells after 3 days of treatment with 0.5 μM buparlisib or alpelisib (A), 10 μM sorafenib (B), or 1 nM palbociclib (C) under adherent culture conditions, followed by plating in conditions for spheroid growth in the presence of 10 nM GC-1 for 7 days. GC-1 alone and each therapeutic agent significantly blocked sphere formation in all cell types. GC-1 in addition to each therapeutic agent further inhibited or completely blocked sphere formation. Significance (* $p<0.05$) was determined by two-way ANOVA followed by Sidak's multiple comparisons test; 3 independent experiments were performed per each treatment group; n=3 per analyses.

199 ATC cells were treated with the indicated inhibitor or vehicle for three days,
200 followed by re-plating in non-adherent conditions. We again observed that GC-1 alone
201 could reduce thyrosphere formation in unmodified ATC cell lines (**Fig. 5A-C**). None of the
202 inhibitors could completely prevent thyrosphere outgrowth when used alone; however,
203 Sorafenib was the most effective overall (**Fig. 5C**). The addition of GC-1 upon removal of

204 each inhibitor blocked nearly all thyrosphere outgrowth. This effect was consistent across
205 all four cell lines and all three inhibitors used. This suggests that GC-1 may be particularly
206 effective at blocking cancer stem cell expansion.

207 **GC-1 promotes re-differentiation of ATC cell lines.**

208 In transduced cells, TRβ activation with T_3 reduces the aggressive phenotype
209 partially through re-differentiation. Therefore, we investigated the potential for GC-1 to
210 promote re-differentiation in parental SW1736 cells. Gene expression analysis using RT-
211 qPCR revealed that 24 hours of GC-1 exposure increased levels of thyroid-specific gene
212 transcripts (**Fig. 6A**). This transcriptomic program is summarized by the thyroid
213 differentiation score (TDS), which significantly increased in GC-1-treated cells (**Fig. 6B**).
214 Additionally, GC-1 alone decreased the overall number of $CD24^-/CD44^+$ cells present in
215 the monolayer population as evident by RT-qPCR (**Sup. Fig. 1A**). We also observed a
216 decrease in the ATC markers *ALCAM* (CD166) and *ALDH1A1* (**Sup. Fig. 1B**).

217 Intriguingly, *SLC5A5* expression was increased with 24 hours of GC-1 (**Fig. 6A**).
218 Therefore, we further investigated NIS protein levels after 48 hours of GC-1 treatment.
219 Both nascent and mature (glycosylated) NIS protein significantly increased following GC-
220 1 treatment (**Fig. 6C-D**). Iodide uptake into cells also increased (**Fig. 6E**), indicating that
221 the increased NIS protein was functional. These findings reveal a novel function of GC-1

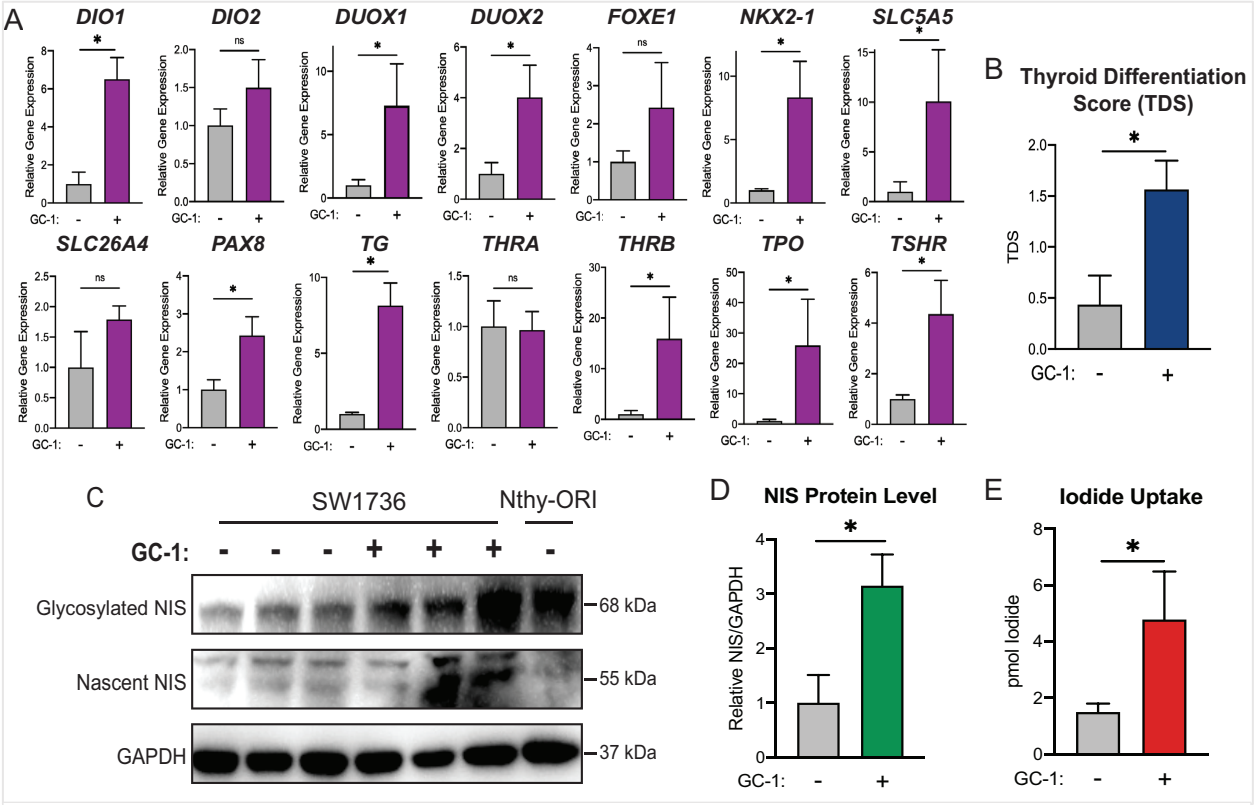

Figure 6. GC-1 induces expression of redifferentiation markers in SW1736 cells. A. RT-qPCR for thyroid differentiation markers was performed on SW1736 cells treated with or without 10 nM GC-1 for 24 hours. mRNA levels in cells treated with GC-1 are relative to the untreated cells. Significance (* $p<0.05$) was determined by Student's unpaired t test; 3 independent experiments were performed per treatment group. B. Thyroid differentiation score (TDS) was calculated using the expression level of the genes in panel A, excluding *THRB*, as previously described (10, 17). Significance (* $p<0.0001$) was determined by Student's unpaired t test. C. SW1736 cells were treated with or without 10 nM GC-1 in triplicate for 48 hours prior to protein extraction and analysis via immunoblot. Normal-like thyroid Nthy-ORI cells were used as a positive control. D. Relative NIS/GAPDH protein levels from (C) were quantified via ImageJ, and significance (* $p<0.01$) was determined by Student's unpaired t test. E. Iodide uptake was measured after 48 hours of GC-1 treatment. Significance was determined by Student's unpaired t test. (* $p<0.001$).

222 to induce re-differentiation in an ATC cell line model and offers a promising target to
223 increase NIS levels and iodide uptake.

224 **GC-1 blunts tumor growth as effectively as Sorafenib *in vivo.***

225 To validate our cell-based findings *in vivo*, the effect of GC-1 alone or in
226 combination with Sorafenib was tested in a xenograft study. GC-1 blunted tumor growth
227 with no significant change in tumor volume over the treatment period similar to Sorafenib
228 and the combination of both treatments (Fig. 7A). At day 16 of treatment, GC-1 induced
229 a significant 60% reduction in tumor mass as did Sorafenib (Fig. 7B, C). The potential for
230 drug synergy was masked due to the equivalent efficacy with Sorafenib at these doses
231 (7A-C). Of note, All mouse groups exhibited similar weight gains over the course of
232 treatment (Fig. 7D). Immunofluorescence image analysis (HALO) on excised tumors
233 revealed diminished Ki67 in all treatment groups (Fig. 7E-F). The combination of GC-1
234 and Sorafenib resulted in a significant reduction in Ki67 expression (Fig. 7F). Region of
235 Interest (ROI) analysis revealed distribution of Ki67 expression preferential in cells along
236 the periphery of the tumor samples.

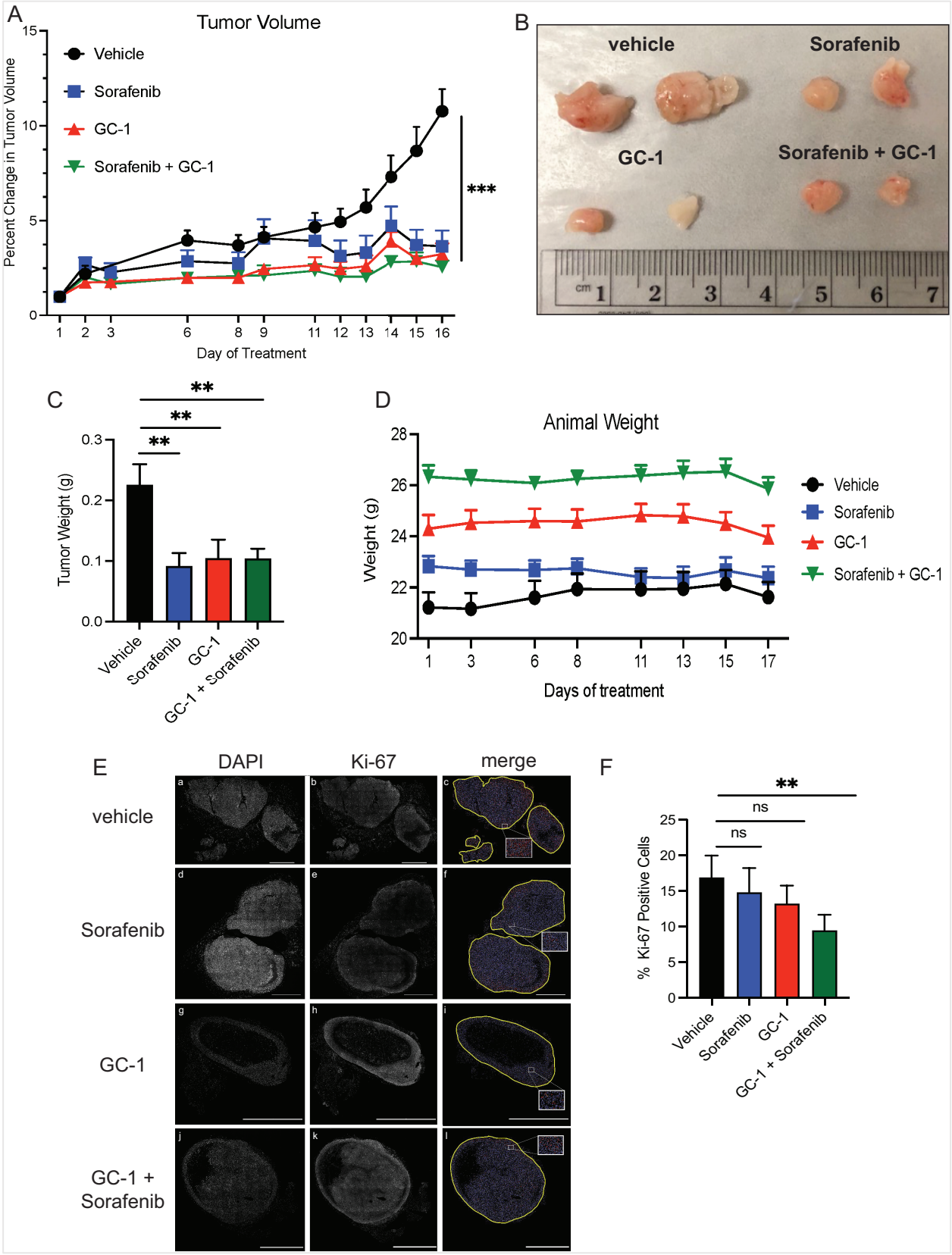
A
Tumor Volume
Vehicle
Sorafenib
GC-1
Sorafenib + GC-1
Percent Change in Tumor Volume
Day of Treatment
***
B
vehicle
Sorafenib
GC-1
Sorafenib + GC-1
C
Tumor Weight (g)
Vehicle
Sorafenib
GC-1
GC-1 + Sorafenib
D
Animal Weight
Weight (g)
Days of treatment
Vehicle
Sorafenib
GC-1
Sorafenib + GC-1
E
DAPI
Ki-67
merge
vehicle
Sorafenib
GC-1
GC-1 + Sorafenib
F
% Ki-67 Positive Cells
ns
Vehicle
Sorafenib
GC-1
GC-1 + Sorafenib

Figure 7. GC-1 inhibits tumor growth as effectively as Sorafenib in an ATC xenograft model. Nude mice were injected subcutaneously with 1 x 10^6 8505C cells. Tumors were established after 1 week. Mice were assigned to 4 treatment groups by weight and injected i.p. daily for 16 days with vehicle control, 10 mg/kg sorafenib, 0.3 mg/kg GC-1, or a combination of sorafenib and CP. (A) Percent change in tumor volumes from day 1 of treatment; *** $p<0.001$ (B) Representative excised tumors from each treatment. No evidence of metastases was noted in any group. Reduced vascularization was observed with GC-1 treatment. (C) Tumors were excised on Day 16 and weighed. Sorafenib (blue), GC-1 (red) induced a 60% reduction in final tumor mass with no difference between the two treatments. The combined treatments did not further reduce the tumor mass over the time period. Significance indicated ** $p<0.01$. (D) Mice were weighed three times a week following drug injections to monitor toxicity. No significant change in animal weight was noted for any group. (E) Representative images of tumors stained for Ki-67 are illustrated. Regions of interest containing only tumor tissue were outlined on each tiled image. Nuclear detection was set to the DAPI channel and the nuclear detection settings were optimized to accurately segment nuclei in the images. (F) Images were analyzed using HALO image analysis (Indica Labs, Albuquerque NM; version 3.3.45) utilizing the HighPlex FL module (version 4.1.3). Quantification of Ki-67 fluorescent intensity per cell is summarized. Sorafenib and GC-1 decreased Ki-67 but only significantly in combination; **$p<0.01$.

DISCUSSION

There is compelling evidence that loss of expression of TRβ, a member of the thyroid hormone receptor (TR) family, through genomic modifications and epigenetic silencing is characteristic of thyroid tumors (3,30-35). Numerous pre-clinical studies demonstrate the potent anti-tumorigenic effect of robust expression of the *THRB* gene. Re-expression of silenced TRβ using demethylating agents delays thyroid tumor progression *in vivo* (36), mice expressing a c-terminal frameshift of TRβ ($Thrb^{PV}$) spontaneously develop follicular thyroid cancer (37), and $Thrb^{PV/PV}$ $Kras^{G12D}$ mice develop thyroid tumors with features of de-differentiated thyroid cancer (38). Our studies in anaplastic thyroid cancer cells revealed that activation of TRβ induces a tumor suppression transcriptomic program, re-differentiation, and reduces the aggressive phenotype (2,10).

Activation of TRβ in pre-clinical and clinical studies have yielded exciting results

251 with great promise for novel interventions. Patients who were rendered hypothyroxinemic
252 and treated with T_3 had longer survival with end-stage solid tumors (39) and T_3 treatment
253 enhanced chemosensitivity (40). Following tyrosine kinase inhibitor therapy, patients
254 demonstrated improved survival with treatment of hypothyroidism (41). Agonists have
255 been developed to target tissue-specific expression of the most abundant TR isomers
256 (42). Mimetics of T_3 that selectively act as TRβ agonists have been clinically successful
257 for treatment of metabolic disorders, hyperlipidemia, hypercholesterolemia, and non-
258 alcoholic steatohepatitis without the harmful cardiovascular effects mediated by TRα
259 (16,17). Our findings demonstrate that GC-1 alone decreases the ATC aggressive
260 phenotype in transduced cells in which TRβ is re-expressed and parental cell lines with
261 diverse genetic backgrounds. These results emphasize the generalizability of GC-1 to
262 activate a TRβ tumor suppression program.

263 In ATC tumors, several genetic alterations and disrupted signaling pathways are
264 usually found. Therefore, the aim is to inhibit or disrupt multiple pathways with
265 combination therapies that block cell survival and proliferation (27,43). In this study, we
266 tested representative drugs that target the MAPK, PI3K, and cell cycle pathways to
267 assess whether GC-1 could increase their effectiveness. Since we have demonstrated
268 that activation of TRβ in ATC represses the PI3K pathway through genomic mechanisms
269 (2,29), GC-1 with either Buparlisib or Alpelisib would be suppressing PI3K activity in
270 concert. In contrast, TRβ does not directly impact MAPK through transcriptomic
271 modulation so GC-1 in combination with Sorafenib demonstrated concordant effects. In
272 all studies, GC-1 reduced the effective concentrations required to observe a reduction in
273 cell viability. One of our most intriguing observations is the impact of GC-1 alone and in

274 combination with inhibitors on cancer stem cell growth in thyrosphere formation. In all
275 ATC cell types, GC-1 alone significantly reduced thyrosphere formation. Remarkably,
276 GC-1 in combination with any of the drug treatments nearly eliminated thyrosphere
277 formation.

278 GC-1 induced re-differentiation in the SW1736 cell line in 24 hours, demonstrating
279 potent transcriptional reprogramming. While we have previously demonstrated the
280 potential for TRβ to promote a more differentiated phenotype in ATC cells, this is the first
281 time we have observed the profound impact of GC-1 in a parental cell line with low TRβ
282 expression. Importantly, we observed a concomitant increase in NIS that led to a higher
283 intake of iodide. Since PDTC and ATC tumors often exhibit a marked decrease in NIS
284 expression and resistance to RAI therapy, the results presented here raise a provocative
285 implication for the use of GC-1 in combination with RAI. Critically, we found that GC-1
286 could blunt tumor growth as effectively as Sorafenib in a xenograft study confirming the
287 observations in cell-based studies. The combination of GC-1 and Sorafenib did not further
288 reduce the tumor volume or mass over the study period. Future studies establishing the
289 pharmacodynamics of GC-1 in combination with different doses of therapeutic agents will
290 elucidate the most effective combinatorial paradigm.

291 Our findings demonstrate that selective activation of TRβ with GC-1 can reduce
292 the aggressive phenotype, reduce the cancer stemness in ATC cells, increase the
293 sensitivity of these cells to therapeutic agents, and promote re-differentiation and iodide
294 uptake. Moreover, GC-1 treatment is as effective as the therapeutic Sorafenib in inhibiting
295 tumor growth. These studies provide the foundation for further investigation of the broad
296 impact of GC-1 on mitigating tumor progression, toxicity, and development of resistance

297 to treatment.

298 **MATERIALS AND METHODS**

299 **Culture of thyroid cell lines.** Anaplastic thyroid cancer cell lines (SW1736, 8505C,
300 OCUT-2, and KTC-2) and the normal-like thyroid cell line Nthy-ORI were cultured in RPMI
301 1640 growth media with L-glutamine (300 mg/L), sodium pyruvate and nonessential
302 amino acids (1%) (Corning), supplemented with 10% fetal bovine serum (Peak Serum)
303 and penicillin-streptomycin (200 IU/L) (Corning) at 37°C, 5% CO_2, and 100% humidity.
304 SW1736-EV and SW-TRβ cells were modified by lentiviral transduction as recently
305 described (10). SW1736, KTC-2, and Nthy-ORI were authenticated by the Vermont
306 Integrative Genomics Resource at the University of Vermont using short tandem repeat
307 profiles (SW1736, May 2019; KTC-2, October 2019; Nthy-ORI, August 2020). 8505C and
308 OCUT2 were authenticated by the University of Colorado using short tandem repeat
309 profiles (8505C, June 2013; OCUT-2, June 2018).

310 **Pharmacological agents.** T_3 and GC-1 (Sigma-Aldrich) were suspended in 1 M NaOH
311 (T_3) and 100% ethanol (GC-1) for stock concentrations of 1 mM before further dilution in
312 culture medium. Buparlisib, Sorafenib, Palbociclib, and Alpelisib (MedChemExpress)
313 were suspended in 100% DMSO for stock concentrations of 50-150 mM before further
314 dilution in culture medium.

315 **Cell Growth and Viability Assays.** Cell growth was measured by cell counting at
316 discrete time points. Cells were seeded in 12- well plates, then treated with GC-1,
317 Buparlisib, Alpelisib, Palbociclib, or Sorafenib to establish time and concentration effects
318 of therapeutics on cell growth. Cell viability was determined by a Sulforhodamine B assay

319 (Abcam) following the manufacturer's protocol. In brief, ATC cells were plated in 96-well
320 clear flat-bottom plates at a density of 5,000 cells per well. Cells were fixed, stained, and
321 imaged using a plate reader according to manufacturer's instructions.

322 **Migration Assay.** Cell migration was determined by wound healing assay as previously
323 described (10, 18). Media was supplemented with GC-1 (10 nM) with and without 0.5 μM
324 Buparlisib, 0.5 μM Alpelisib, 1 nM Palbociclib, or 5 μM Sorafenib. Images were obtained
325 at 0, 16, 24, 48, and 72 hours or until 100% wound closure, depending on the cell line.
326 Percent closure was calculated relative to the area of the initial scratch.

327 **Tumorsphere Assay.** Tumorspheres formed from ATC cells were used to assess self-
328 renewal and sphere-forming efficiency as previously described (10). Where indicated,
329 adherent cells were treated with 0.5 μM Buparlisib, 0.5 μM Alpelisib, 1 nM Palbociclib, 5
330 μM Sorafenib, or vehicle for 72 hours prior to tumorsphere-forming assay. Tumorspheres
331 were then cultured in with or without GC-1 (10 nM) to evaluate the effects of liganded TRβ
332 on thyrosphere growth alone or after treatment with a therapeutic agent.

333 **Western blot Analysis.** Proteins were isolated from whole cells in lysis buffer and
334 visualized by Western blot as previously described (9, 10, 18). Specific proteins were
335 detected with the indicated antibodies (Table 1); immunoreactive proteins were detected
336 by enhanced chemiluminescence (Thermo Fisher Scientific) on a ChemiDoc XRS+ (Bio-
337 Rad Laboratories).

338 **RNA Extraction and Quantitative Real-Time PCR (qRT-PCR).** Total RNA was
339 extracted using RNeasy Plus Kit (Qiagen) according to manufacturer's protocol. cDNA

340 was generated using 5X LunaScript RT SuperMix, and mRNA expression was quantified
341 by qRT-PCR using 2X Luna Universal qPCR Master Mix (New England Biolabs) on a
342 QuantStudio 3 real-time PCR system (Applied Biosystems). Fold change in gene
343 expression compared to housekeeping controls was calculated using the ddCT method.
344 Primer sequences are indicated in Table 2.

345 **Iodide Uptake Assay.** Cells were seeded at a density of 40,000 cells per well in a 96 well
346 plate with or without 10 nM GC-1 for 48 hours. Media was discarded, and cells were
347 washed four times with warm PBS before incubation with 1 μM potassium iodide (KI,
348 Sigma-Aldrich) in PBS for 1 hour at 37°C. Wells were washed an additional four times
349 with warm PBS and 100 μL of ddH_2O were added to each well. 100 μl of 24 mM
350 ammonium cerium (IV) sulfate hydrate with 5.7% concentrated H_2SO_4 (Sigma-Aldrich)
351 and 100 μl of 24 mM sodium arsenite (III) with 205 mM sodium chloride (NaCl) and 50
352 mM sodium hydroxide (NaOH, Sigma-Aldrich) were added to each well. Plates were
353 incubated in the dark at room temperature for 30 minutes, and absorbance at 415 nm
354 was measured with a Synergy 2 Multi-Detection Microplate Reader (Agilent
355 Technologies).

356 ***In Vivo* Evaluation of Sobetirome (GC-1) and Sorafenib. T**he xenograft experiment
357 was approved by the Animal Care and Use Committee of the University of Vermont
358 (Protocol X0-018). Four-week-old athymic female nude mice (outbred homozygous nude
359 *Foxn1*^{nu}/*Foxn1*^{nu}) were purchased from Jackson Laboratory (Bar Harbor, ME, USA) and
360 were allowed to acclimatize for one week. Mice were given food and water *ad libitum*.
361 Mice were anesthetized using 3% isoflurane delivered at 1.5 L/min, and tumors were

362 established by subcutaneously injecting 1 x 10^6 8505C cells with a 26G needle in 100 μL
363 of high concentration Matrigel (Corning Inc.) diluted 1:2 with base RPMI-1640 into each
364 flank of 24 mice. One week later, mice were sorted into four treatment groups to achieve
365 approximately equal body weights within each group. Mice were then administered 0.3
366 mg/kg GC-1, 10 mg/kg Sorafenib, both GC-1 and Sorafenib, or vehicle control every day
367 via intraperitoneal injection using 27G needles. Pharmacological agents were dissolved
368 in 100% DMSO and diluted daily in 30% DMSO, 40% PEG300, and 30% PBS and
369 incubated at 55°C for 10 minutes prior to vortexing to encourage complete solubilization.
370 Tumor dimensions were measured with digital calipers, and the volumes were calculated
371 by the following formula: $(\Pi \times a \times b^2) / 6$, where a represents the largest diameter and b
372 is the perpendicular diameter. The body weight of each animal was taken at least twice a
373 week to measure toxicity. After treatment for 16 days, mice were euthanized with carbon
374 dioxide, and the tumors were harvested, fixed with formalin (Thermo Fisher Scientific),
375 and stored at 4°C prior to slide sectioning and immunohistochemistry.

376 **Immunofluorescent Analysis of Tumor Tissues.** Formalin fixed paraffin embedded
377 human thyroid xenograft tumor blocks were sectioned at 5 μm thickness onto glass
378 microscope slides, dried overnight, and then baked at 60°C for one hour. Sections were
379 deparaffinized in three changes of xylene for 15 minutes each, then dehydrated in a series
380 of graded ethanols (100% x2, 95% x2, 70%, 50%, water) for 5 minutes each. Antigen
381 retrieval utilizing 1X DAKO target Retrieval Solution (DAKO product #S1699, lot#
382 11270951; Agilent Technologies, Santa Clara, CA) in 50% glycerol was performed in a
383 Decloaking Chamber (SP1 - 100°C for 15 min, SP2 - 90°C for 1 min). Following antigen
384 retrieval, slides were cooled to room temperature in the antigen retrieval solution for 20

385 minutes. Slides were then rinsed 2x 5 minutes in distilled water followed by 0.2% Tween-
386 20 for an additional 5 minutes. Tissue sections were blocked for non-specific antibody
387 reactivity by incubation with 10% normal goat serum diluted in phosphate buffered saline
388 (PBS)/ 3% bovine serum albumin (BSA)/ 0.3% Triton X-100 for 60 minutes at room
389 temperature. Immediately following blocking, slides were incubated with rabbit polyclonal
390 anti-KI-67 (Abcam, Cambridge, UK; #ab15580) at a concentration 1.4 µg/ml in PBS/3.0%
391 BSA/0.3% Triton X-100 overnight at 4°C. Slides were then rinsed 7x 5 minutes in
392 PBS/3.0% BSA and incubated with goat anti-rabbit Alexa 488 conjugated secondary
393 antibody (ThermoFisher, Waltham MA; #A11008) in PBS/3.0% BSA for 60 minutes at
394 room temperature. Staining was followed by 5x 5 minute rinses with PBS/3.0% BSA.
395 Samples were counterstained with 4', 6-diamidino-2-phenylindole (DAPI) (ThermoFisher,
396 #D1306) at a concentration of 10 µg/ml in PBS / 3.0%BSA for 15 minutes then rinsed 3x
397 5 minutes in distilled water. Following rinses slides were mounted with a #1.5 coverslip
398 and DAKO IF mounting media (Agilent; #S3023) for imaging.

399 **Confocal Imaging of human thyroid xenograft tissue.** Xenograft samples stained with
400 anti-KI-67 and DAPI were imaged on a Nikon A1R HD point scanning confocal
401 microscope with a 20x Plan Apo λ DIC objective lens (NA 0.75, WD 1000 µm) with 488
402 nm and 405 nm laser excitation respectively. Image acquisition was completed in
403 galvanometic scanning mode (Nikon Instruments Inc., Melville NY). Images of the entire
404 xenograft section were acquired at 12-bit resolution using the tile scan function. Images
405 were saved in ND2 file format in NIS Elements (version 5.2.1, Nikon, Tokyo, Japan).

406 **Indica Labs HALO Image Analysis.** Images were analyzed using HALO image analysis
407 (Indica Labs, Albuquerque NM; version 3.3.45) utilizing the HighPlex FL module (version

408 4.1.3). Regions of interest containing only tumor tissue were outlined on each tiled
409 image. Nuclear detection was set to the DAPI channel and the nuclear detection settings
410 were optimized to accurately segment nuclei in the images. Membrane and cytoplasmic
411 threshold settings were optimized for Ki-67 staining in the Alexa 488 (green) channel.
412 Cytoplasmic detection settings were set to 4095 (in a 12 bit image) so that no cytoplasmic
413 background staining would be included in the analysis. Nuclear positive signal setting
414 threshold was set per image, to most accurately reflect the antibody staining level
415 observed in the image. Percent Ki-67 positive cells were summarized.

416 **Ethics statement and animal modeling.** All animal procedures were approved by
417 Institutional Animal Care and Use Committee (IACUC) at the University of Vermont. All
418 animals were maintained in pathogen-free conditions and cared for in accordance with
419 IACUC policies and certification. All surgeries were performed with isoflurane anesthesia.
420 Temperature-controlled post-surgical monitoring was implemented to minimize suffering.
421 Mice carrying anaplastic thyroid tumors were euthanized at designated time points for
422 tumor collection. We used signs of ulceration or a maximum individual tumor size of 2000
423 mm^3 as a protocol-enforced endpoint.

424 **Statistics.** All statistical analyses were performed using GraphPad Prism 9.3.1 and
425 assumed that variance was similar between experimental groups. Sample sizes were a
426 minimum of three independent experiments. Paired comparisons were conducted by
427 unpaired Student's t-test assuming two-tailed distribution. Group comparisons were made
428 by one-way ANOVA followed by Sidak's or Tukey's multiple comparison test as
429 appropriate. Two-way ANOVA followed by a Tukey's multiple comparison test was

430 conducted for multigroup analysis. Data are represented as mean ± standard deviation
431 or standard error of the mean where indicated. Differences were considered statistically
432 significant at $p \leq 0.05$ (*$p \leq 0.05$, **$p \leq 0.01$, ***$p \leq 0.001$). Area under the curve (AUC) at
433 the 95th confidence interval was used to evaluate statistical differences in growth and
434 migration assays.

435 **ACKNOWLEDGEMENTS:**

436 The research reported here was supported by grants from National Institutes of Health
437 U54 GM115516 for the Northern New England Clinical and Translational Research
438 Network; National Cancer Institute 1F99CA245796-01; UVM Cancer Center-Lake
439 Champlain Cancer Research Organization (C3) 12577-21; and UVM Larner College of
440 Medicine. SW1736 and KTC-2 cell lines were generously provided by Dr. John Copland
441 III (Mayo Clinic). Human cell line authentication, NextGen sequencing, automated DNA
442 sequencing and molecular imaging was performed in the Vermont Integrative Genomics
443 Resource supported by the University of Vermont Cancer Center, Lake Champlain
444 Cancer Research Organization, and the UVM Larner College of Medicine. Additional
445 human cell lines 8505C and OCUT-2 were obtained and authenticated from the University
446 of Colordo Cancer Center Tissue Culture Shared Resource supported by National Cancer
447 Institute P30CA046934. Immunofluorescence staining, imaging and analysis was
448 performed at the Microscopy Imaging Center at the University of Vermont (RRID#
449 SCR_018821). Confocal microscopy was performed on a Nikon A1R-HD point scanning
450 confocal microscope supported by NIH award number 1S10OD025030-01 from the Office
451 of Research Infrastructure Programs. We thank the Histology Research Support Facility
452 for histological services in the Department of Pathology and Laboratory Medicine at the

University of Vermont Medical Center, Burlington, VT. We thank the Office of Animal Care Management for their expertise for *in vivo* experiments.

Authors' Contribution Statement: NEG: Conceptualization, Formal analysis, Investigation, Writing – Review & editing. **LMC:** Formal analysis, Investigation, Writing. **ERW:** Formal analysis, Investigation. **JAT:** Investigation, Writing – Review & editing. **ELB:** Conceptualization, – Review & editing. **FEC:** Conceptualization, Resources, Writing-Review & editing, Supervision, Project administration, Funding acquisition.

Authors' Disclosure Statement: The authors declare they have no conflict of interest.

Funding Statement: The research reported here was supported by grants from National Institutes of Health U54 GM115516 for the Northern New England Clinical and Translational Research Network; National Cancer Institute 1F99CA245796-01; UVM Cancer Center-Lake Champlain Cancer Research Organization (C3) 12577-21; and UVM Larner College of Medicine.

REFERENCES

1. Kim WG, Cheng SY. Thyroid hormone receptors and cancer. Biochim Biophys Acta **2013**;1830(7):3928-36 doi 10.1016/j.bbagen.2012.04.002.
2. Bolf EL, Gillis NE, Davidson CD, Rodriguez PD, Cozzens L, Tomczak JA*, et al.* Thyroid Hormone Receptor Beta Induces a Tumor-Suppressive Program in Anaplastic Thyroid Cancer. Mol Cancer Res **2020**;18(10):1443-52 doi 10.1158/1541-7786.MCR-20-0282.
3. Aranda A, Martinez-Iglesias O, Ruiz-Llorente L, Garcia-Carpizo V, Zambrano A. Thyroid receptor: roles in cancer. Trends in endocrinology and metabolism: TEM **2009**;20(7):318-24 doi 10.1016/j.tem.2009.03.011.
4. Kim WG, Zhao L, Kim DW, Willingham MC, Cheng SY. Inhibition of tumorigenesis by the thyroid hormone receptor beta in xenograft models. Thyroid **2014**;24(2):260-9 doi 10.1089/thy.2013.0054.
5. Kowalik MA, Puliga E, Cabras L, Sulas P, Petrelli A, Perra A*, et al.* Thyroid hormone inhibits hepatocellular carcinoma progression via induction of differentiation and metabolic reprogramming. J Hepatol **2020**;72(6):1159-69 doi 10.1016/j.jhep.2019.12.018.

482 6. Zhu L, Tian G, Yang Q, De G, Zhang Z, Wang Y*, et al.* Thyroid hormone receptor β1 suppresses
483 proliferation and migration by inhibiting PI3K/Akt signaling in human colorectal cancer cells.
484 Oncol Rep **2016**;36(3):1419-26 doi 10.3892/or.2016.4931.
485 7. Bolf EL, Gillis NE, Davidson CD, Cozzens LM, Kogut S, Tomczak JA*, et al.* Common tumor-
486 suppressive signaling of thyroid hormone receptor beta in breast and thyroid cancer cells. Mol
487 Carcinog **2021**;60(12):874-85 doi 10.1002/mc.23352.
488 8. López-Mateo I, Alonso-Merino E, Suarez-Cabrera C, Park JW, Cheng SY, Alemany S*, et al.* Thyroid
489 Hormone Receptor β Inhibits Self-Renewal Capacity of Breast Cancer Stem Cells. Thyroid
490 **2020**;30(1):116-32 doi 10.1089/thy.2019.0175.
491 9. Martínez-Iglesias O, Ruiz-Llorente L, Jurado CC, Aranda A. Chapter 11 - Thyroid Hormone
492 Receptors and their Role in Cell Proliferation and Cancer. In: Ulloa-Aguirre A, Tao Y-X, editors.
493 Cellular Endocrinology in Health and Disease (Second Edition). Boston: Academic Press; 2021. p
494 229-46.
495 10. Carr FE, Tai PW, Barnum MS, Gillis NE, Evans KG, Taber TH*, et al.* Thyroid Hormone Receptor-
496 beta (TRbeta) Mediates Runt-Related Transcription Factor 2 (Runx2) Expression in Thyroid
497 Cancer Cells: A Novel Signaling Pathway in Thyroid Cancer. Endocrinology **2016**;157(8):3278-92
498 doi 10.1210/en.2015-2046.
499 11. Pourvali K, Shimi G, Ghorbani A, Shakery A, Shirazi FH, Zand H. Selective thyroid hormone
500 receptor beta agonist, GC-1, is capable to reduce growth of colorectal tumor in syngeneic mouse
501 models. J Recept Signal Transduct Res **2022**:1-8 doi 10.1080/10799893.2022.2032748.
502 12. Davidson CD, Gillis NE, Carr FE. Thyroid Hormone Receptor Beta as Tumor Suppressor: Untapped
503 Potential in Treatment and Diagnostics in Solid Tumors. Cancers (Basel) **2021**;13(17) doi
504 10.3390/cancers13174254.
505 13. Lee WK, Cheng SY. Targeting transcriptional regulators for treatment of anaplastic thyroid
506 cancer. J Cancer Metastasis Treat **2021**;7 doi 10.20517/2394-4722.2021.58.
507 14. Nabhan F, Dedhia PH, Ringel MD. Thyroid cancer, recent advances in diagnosis and therapy. Int J
508 Cancer **2021**;149(5):984-92 doi 10.1002/ijc.33690.
509 15. Saponaro F, Sestito S, Runfola M, Rapposelli S, Chiellini G. Selective Thyroid Hormone Receptor-
510 Beta (TRβ) Agonists: New Perspectives for the Treatment of Metabolic and Neurodegenerative
511 Disorders. Front Med (Lausanne) **2020**;7:331 doi 10.3389/fmed.2020.00331.
512 16. Trost SU, Swanson E, Gloss B, Wang-Iverson DB, Zhang H, Volodarsky T*, et al.* The thyroid
513 hormone receptor-beta-selective agonist GC-1 differentially affects plasma lipids and cardiac
514 activity. Endocrinology **2000**;141(9):3057-64 doi 10.1210/endo.141.9.7681.
515 17. Grover GJ, Mellstrom K, Ye L, Malm J, Li YL, Bladh LG*, et al.* Selective thyroid hormone receptor-
516 beta activation: a strategy for reduction of weight, cholesterol, and lipoprotein (a) with reduced
517 cardiovascular liability. Proc Natl Acad Sci U S A **2003**;100(17):10067-72 doi
518 10.1073/pnas.1633737100.
519 18. Kelly MJ, Pietranico-Cole S, Larigan JD, Haynes NE, Reynolds CH, Scott N*, et al.* Discovery of 2-
520 [3,5-dichloro-4-(5-isopropyl-6-oxo-1,6-dihydropyridazin-3-yloxy)phenyl]-3,5-dio xo-2,3,4,5-
521 tetrahydro[1,2,4]triazine-6-carbonitrile (MGL-3196), a Highly Selective Thyroid Hormone
522 Receptor beta agonist in clinical trials for the treatment of dyslipidemia. J Med Chem
523 **2014**;57(10):3912-23 doi 10.1021/jm4019299.
524 19. Elbers LP, Kastelein JJ, Sjouke B. Thyroid Hormone Mimetics: the Past, Current Status and Future
525 Challenges. Curr Atheroscler Rep **2016**;18(3):14 doi 10.1007/s11883-016-0564-7.
526 20. Siegel RL, Miller KD, Jemal A. Cancer Statistics, 2017. CA Cancer J Clin **2017**;67(1):7-30 doi
527 10.3322/caac.21387.

528 21. Pereira M, Williams VL, Hallanger Johnson J, Valderrabano P. Thyroid Cancer Incidence Trends in
529 the United States: Association with Changes in Professional Guideline Recommendations.
530 Thyroid **2020**;30(8):1132-40 doi 10.1089/thy.2019.0415.
531 22. Glaser SM, Mandish SF, Gill BS, Balasubramani GK, Clump DA, Beriwal S. Anaplastic thyroid
532 cancer: Prognostic factors, patterns of care, and overall survival. Head Neck **2016**;38 Suppl
533 1:E2083-90 doi 10.1002/hed.24384.
534 23. Prasongsook N, Kumar A, Chintakuntlawar AV, Foote RL, Kasperbauer J, Molina J*, et al.* Survival
535 in Response to Multimodal Therapy in Anaplastic Thyroid Cancer. J Clin Endocrinol Metab
536 **2017**;102(12):4506-14 doi 10.1210/jc.2017-01180.
537 24. Subbiah V, Kreitman RJ, Wainberg ZA, Cho JY, Schellens JHM, Soria JC*, et al.* Dabrafenib and
538 Trametinib Treatment in Patients With Locally Advanced or Metastatic BRAF V600-Mutant
539 Anaplastic Thyroid Cancer. J Clin Oncol **2018**;36(1):7-13 doi 10.1200/JCO.2017.73.6785.
540 25. De Leo S, Trevisan M, Fugazzola L. Recent advances in the management of anaplastic thyroid
541 cancer. Thyroid Res **2020**;13(1):17 doi 10.1186/s13044-020-00091-w.
542 26. Gentile D, Orlandi P, Banchi M, Bocci G. Preclinical and clinical combination therapies in the
543 treatment of anaplastic thyroid cancer. Med Oncol **2020**;37(3):19 doi 10.1007/s12032-020-
544 1345-2.
545 27. Molinaro E, Romei C, Biagini A, Sabini E, Agate L, Mazzeo S*, et al.* Anaplastic thyroid carcinoma:
546 from clinicopathology to genetics and advanced therapies. Nature Reviews Endocrinology
547 **2017**;13:644 doi 10.1038/nrendo.2017.76.
548 28. Landa I, Ibrahimpasic T, Boucai L, Sinha R, Knauf JA, Shah RH*, et al.* Genomic and transcriptomic
549 hallmarks of poorly differentiated and anaplastic thyroid cancers. The Journal of Clinical
550 Investigation **2016**;126(3):1052-66 doi 10.1172/JCI85271.
551 29. Davidson CD, Bolf EL, Gillis NE, Cozzens LM, Tomczak JA, Carr FE. Thyroid hormone receptor beta
552 inhibits the PI3K-Akt-mTOR signaling axis in anaplastic thyroid cancer cell lines via genomic
553 mechanisms. Journal of the Endocrine Society **2021** doi 10.1210/jendso/bvab102.
554 30. Silva JM, Domínguez G, González-Sancho JM, García JM, Silva J, García-Andrade C*, et al.*
555 Expression of thyroid hormone receptor/erbA genes is altered in human breast cancer.
556 Oncogene **2002**;21:4307 doi 10.1038/sj.onc.1205534.
557 31. Kim W, Cheng S. Thyroid hormone receptors and cancer. Volume 1830. Biochim Biophys
558 Acta2013. p 3928-36.
559 32. Jezequel P, Campone M, Gouraud W, Guerin-Charbonnel C, Leux C, Ricolleau G*, et al.* bc-
560 GenExMiner: an easy-to-use online platform for gene prognostic analyses in breast cancer.
561 Breast Cancer Res Treat **2012**;131(3):765-75 doi 10.1007/s10549-011-1457-7.
562 33. Jezequel P, Frenel JS, Campion L, Guerin-Charbonnel C, Gouraud W, Ricolleau G*, et al.* bc-
563 GenExMiner 3.0: new mining module computes breast cancer gene expression correlation
564 analyses. Database (Oxford) **2013**;2013:bas060 doi 10.1093/database/bas060.
565 34. Wojcicka A, Piekielko–Witkowska A, Kedzierska H, Rybicka B, Poplawski P, Boguslawska J*, et al.*
566 Epigenetic Regulation of Thyroid Hormone Receptor Beta in Renal Cancer. PLOS ONE
567 **2014**;9(5):e97624 doi 10.1371/journal.pone.0097624.
568 35. Park JW, Zhao L, Willingham M, Cheng S-y. Oncogenic mutations of thyroid hormone receptor β.
569 Oncotarget **2015**;6(10):8115-31.
570 36. Kim WG, Zhu X, Kim DW, Zhang L, Kebebew E, Cheng SY. Reactivation of the silenced thyroid
571 hormone receptor beta gene expression delays thyroid tumor progression. Endocrinology
572 **2013**;154(1):25-35 doi 10.1210/en.2012-1728.
573 37. Suzuki H, Willingham MC, Cheng SY. Mice with a mutation in the thyroid hormone receptor beta
574 gene spontaneously develop thyroid carcinoma: a mouse model of thyroid carcinogenesis.
575 Thyroid **2002**;12(11):963-9 doi 10.1089/105072502320908295.

576 38. Zhu X, Zhao L, Park JW, Willingham MC, Cheng SY. Synergistic signaling of KRAS and thyroid
577 hormone receptor beta mutants promotes undifferentiated thyroid cancer through MYC up-
578 regulation. Neoplasia **2014**;16(9):757-69 doi 10.1016/j.neo.2014.08.003.
579 39. Hercbergs A, Johnson RE, Ashur-Fabian O, Garfield DH, Davis PJ. Medically induced euthyroid
580 hypothyroxinemia may extend survival in compassionate need cancer patients: an observational
581 study. Oncologist **2015**;20(1):72-6 doi 10.1634/theoncologist.2014-0308.
582 40. Huang J, Jin L, Ji G, Xing L, Xu C, Xiong X*, et al.* Implication from thyroid function decreasing
583 during chemotherapy in breast cancer patients: chemosensitization role of triiodothyronine.
584 BMC Cancer **2013**;13:334 doi 10.1186/1471-2407-13-334.
585 41. Lechner MG, Vyas CM, Hamnvik OR, Alexander EK, Larsen PR, Choueiri TK*, et al.* Hypothyroidism
586 During Tyrosine Kinase Inhibitor Therapy Is Associated with Longer Survival in Patients with
587 Advanced Nonthyroidal Cancers. Thyroid **2018**;28(4):445-53 doi 10.1089/thy.2017.0587.
588 42. Davis PJ, Tang HY, Hercbergs A, Lin HY, Keating KA, Mousa SA. Bioactivity of Thyroid Hormone
589 Analogs at Cancer Cells. Front Endocrinol (Lausanne) **2018**;9:739 doi 10.3389/fendo.2018.00739.
590 43. Alobuia W, Gillis A, Kebebew E. Contemporary Management of Anaplastic Thyroid Cancer. Curr
591 Treat Options Oncol **2020**;21(10):78 doi 10.1007/s11864-020-00776-2.

592